

## Detection of runaway electrons at the COMPASS tokamak using a Timepix3-based semiconductor detector

S. Kulkov,<sup>a,\*</sup> M. Marcisovsky,<sup>a</sup> P. Svihra,<sup>a</sup> M. Tunkl,<sup>a</sup> M. van Beuzekom,<sup>b</sup> J. Caloud,<sup>a,c</sup> J. Cerovsky,<sup>a,c</sup> O. Ficker,<sup>a,c</sup> E. Macusova,<sup>c</sup> J. Mlynar,<sup>a,c</sup> V. Weinzettl,<sup>c</sup> V. Svoboda<sup>a</sup> and the COMPASS team

<sup>a</sup>Department of Physics, Faculty of Nuclear Sciences and Physical Engineering,  
Czech Technical University in Prague,  
Brehova 78/7, 115 19 Prague, Czech Republic

<sup>b</sup>Nikhef,  
Science Park 105, 1098 XG Amsterdam, Netherlands

<sup>c</sup>Institute of Plasma Physics of the Czech Academy of Sciences,  
Za Slovankou 1782/3, 182 00 Prague, Czech Republic

E-mail: [sergei.kulkov@fjfi.cvut.cz](mailto:sergei.kulkov@fjfi.cvut.cz)

**ABSTRACT:** Runaway electrons are considered dangerous for the integrity of tokamak vacuum vessels. To secure the success of the future tokamak-based machines, reliable diagnostics and mitigation strategies are necessary. The COMPASS tokamak supported the research of runaway electron physics via regular experimental campaigns. During the last two experimental campaigns dedicated to runaway electrons, a semiconductor detector with a Timepix3 readout chip, Si sensor, and the SPIDR readout system was tested. Time evolution signals, energy measurements, and sensor snapshots collected with the Timepix3-based detector are presented.

**KEYWORDS:** X-ray detectors; Plasma diagnostics - charged-particle spectroscopy; Plasma diagnostics - interferometry, spectroscopy and imaging

---

\*Corresponding author.

---

## Contents

<b>1</b>	<b>Introduction</b>	<b>1</b>
<b>2</b>	<b>The COMPASS tokamak</b>	<b>2</b>
<b>3</b>	<b>The Timepix3 detector</b>	<b>3</b>
<b>4</b>	<b>The Timepix3 setup</b>	<b>3</b>
4.1	11th RE campaign: January 2020	3
4.2	12th RE campaign: November 2020	4
<b>5</b>	<b>Experiment results</b>	<b>4</b>
<b>6</b>	<b>Energy measurements and calibration of the Timepix3</b>	<b>8</b>
<b>7</b>	<b>Experiments at the GOLEM tokamak</b>	<b>10</b>
<b>8</b>	<b>Conclusion</b>	<b>10</b>

---

## 1 Introduction

One of the key distinctions of the tokamak configuration in magnetic confinement fusion is the induction of electric current in plasma. While this plays a crucial role as the toroidal electric current generates a poloidal magnetic field necessary to achieve the helicity of magnetic field lines, it also may lead to the generation of so-called runaway electrons (RE). Electrons in the tokamak plasma are constantly accelerated by the toroidal electric field and to a certain limit this is countered by the collisional drag. The critical value of electric field, above which electrons overcome the drag and become runaway, reaching relativistic velocities, is called the Dreicer critical field  $E_D = \frac{e^3 n_e \ln \Lambda (2 + Z_{\text{eff}})}{4\pi \epsilon_0^2 m_e v^2}$ , where  $e$  is the elementary charge,  $n_e$  is the electron density,  $\ln \Lambda$  is the Coulomb logarithm,  $Z_{\text{eff}}$  is the effective ion charge,  $\epsilon_0$  is the vacuum permittivity,  $m_e$  is the electron rest mass, and  $v$  is the electron velocity [1]. REs are one of the key problems future tokamaks have to solve because of high plasma electric currents. While for ITER it is predicted that REs can carry up to 70% of the plasma current [2], on some tokamaks, it has been discovered that up to 80% of the plasma electric current may be converted to RE current [3, 4] with RE energies up to hundreds of MeV [5]. If a RE beam leaves the main plasma volume and reaches the vacuum vessel wall, it may damage the material [6]. In a fusion reactor, where the vacuum vessel walls will be actively cooled, this may lead to a leakage of the coolant.

During the current ramp-up phase of the tokamak discharge, the generation of REs can be avoided with an appropriate fueling scenario [7]. The flat-top phase is safe from REs as long as the plasma density is high enough so that the value of the electric field does not reach the Dreicer critical

field [8]. However, disruptions, which are a series of events that lead to a loss of control of the plasma confined, are most potent in the RE production, as the plasma cools down and the toroidal electric field enhances. The quick cooling of the bulk plasma leads to an incomplete thermalization of the electron velocity distribution, leaving a part of electrons that enter the RE regime. To secure the operation of ITER, a disruption mitigation system (DMS) will be used in all operational scenarios starting from the first pre-fusion operation phase — the second phase of the ITER operational plan [9]. For ITER DMS, a massive material injection system was chosen — the shattered pellet injection (SPI) [10–12]. Massive material injection is used to achieve more isotropic plasma cooling via radiation rather than localized deposition of the energy stored in the plasma via contact with the plasma-facing components.

The experiments on both RE generation and their behavior in tokamak plasmas and RE mitigation systems are ongoing. To support the research, technology from other fields of physics research can be utilized, for example, particle and radiation diagnostics that are widely applied in high-energy particle physics. Semiconductor pixel detectors, which have excellent spatial and temporal resolutions, are a suitable addition to plasma diagnostics. Coming in compact dimensions, these detectors can be placed close to the tokamak vacuum vessel, pinpointing the source of radiation. Sophisticated data readout systems provide multiple types of information about radiation, combining multiple diagnostics into one.

This work presents data collected with a Timepix3-based hybrid semiconductor pixel detector during two RE-dedicated campaigns at the COMPASS tokamak.

## 2 The COMPASS tokamak

From 2008 until 2021, the COMPASS tokamak was larger of the two tokamaks in the Czech Republic. Since 2014, it regularly contributes to the RE research [6]. After the last experimental campaigns in 2021, the installation of the COMPASS tokamak successor — COMPASS Upgrade — will begin [13]. The main parameters of the COMPASS tokamak with ITER-like plasmas can be seen in the table 1.

**Table 1.** Main parameters of the COMPASS tokamak [14].

Major radius	0.56 m
Minor radius	0.23 m
Vacuum pressure	$10^{-6}$ Pa
Plasma current	< 400 kA
Toroidal magnetic field	0.9–1.6 T
Pulse length	$\approx$ 400 ms
NBI heating	$2 \times 0.4$ MW

A rather rich set of diagnostics is involved in RE research at the COMPASS tokamak, including but not limited to: 24 internal Mirnov coils, 16 internal partial Rogowski coils, a pair of NaI(Tl) scintillation detectors for hard X-ray (HXR) measurements with an energy spectrum 50 keV–10 MeV, an EJ-410 fast neutron detector within a 10 cm-thick shield of Pb blocks for detection of neutrons and HXR with energy above 500 keV, fast visible cameras Photron Mini UX100, operated with

frame rates of 2–6 kfps, and Photron SA-X2 with frame rates of  $\sim 30$  kfps [15]. The COMPASS tokamak is also equipped with an MGI (massive gas injection) system and, during both the 11th and 12th RE campaigns, a room temperature solid-state pellet injector was installed and utilized.

### 3 The Timepix3 detector

The Timepix3 readout chip is the second generation in the Timepix series of pixel readout chips for semiconductor and gas chamber detectors [16]. The chip was developed by the Medipix collaboration at CERN and produced in a 130 nm CMOS technology. The key characteristic of the chip is a data-driven readout with a simultaneous recording of the time of particle arrival — or ToA — and the time the signal spends over a preset threshold (used to cut off noise) — time over threshold, or ToT. The chip has a matrix of  $256 \times 256$  pixel channels with a pixel size of  $55 \times 55 \mu\text{m}^2$ . The packet size for each hit is 48 bit, with 16 bits allocated for pixel address, 14 bits for ToA with an addition of 4 bits for further refinement, which provides a 1.5625 ns temporal resolution, 10 bits for ToT, and 4 bits for a header, including a switch between a data-driven and a sequential readout modes. Combining the ToA timestamps, ToT values, and pixel coordinates, the system provides a time evolution, energy spectrograms, and sensor snapshots of the radiation measured. In the pinhole configuration, sensor snapshots allow to pinpoint the source of radiation with good spatial resolution. The readout is dead time-free for hit rates up to  $40 \text{ Mhits s}^{-1} \text{ cm}^{-2}$ .

During the RE-dedicated campaigns at the COMPASS tokamak, a hybrid semiconductor detector with the Timepix3 readout chip and a  $200 \mu\text{m}$ -thick silicon sensor was used (referred to as “the Timepix3 detector” in the further text, see figure 1). The detector was coupled with the SPIDR (Speedy Pixel Detector Readout) readout system developed at Nikhef, Netherlands [17]. The SPIDR system provides additional 16 bits for an extended time window of measurements up to 26.8 seconds from the initial  $409.6 \mu\text{s}$  of the Timepix3 architecture. To achieve complete depletion, the sensor has to be biased to  $-150 \text{ V}$ . During the campaigns, the SPIDR readout system was hosted on a Xilinx Virtex-7 FPGA VC707 board, which also provided a slot for an external trigger. This was utilized to shift the time signal measured by the detector for comparison with the tokamak diagnostics.

Thanks to the pixel matrix, Timepix3 is capable of distinguishing if either a photon, an electron, or a heavier particle is detected based on the number of pixels that the measured particle/radiation quantum has crossed. During the analysis, a general assumption that photons cover up to 3 different pixels was taken into account, based on the probability of photon interaction with  $200 \mu\text{m Si}$ , maximum energy of Compton electrons, and electron CSDA (continuous slowing down approximation) range. Therefore, all figures shown in this work represent only the soft X-ray (SXR) signal.

## 4 The Timepix3 setup

### 4.1 11th RE campaign: January 2020

During the 11th RE campaign conducted in January 2020 at the COMPASS tokamak, the Timepix3 chipboard was installed at the radial midplane port with a length of 740 mm and diameter of 151 mm, which provided a clear view on the high-field side (HFS) of the tokamak vacuum vessel. A lead pinhole was put between the sensor and the port with a Be window on the port as the vacuum barrier. A PCB (Printed-Circuit Board) with an FPGA (Field-Programmable Gate Array), where the SPIDR



**Figure 1.** The Timepix3 chipboard. The black plastic is used to shield the Si sensor, which is bump-bonded to the readout ASIC below the sensor, from stray light. Yellow kapton tape keeps the sensor clean from dust. The hole in the Al layer (used for biasing the sensor) atop the sensor was cut out for experiments with a laser at Nikhef.

software was installed, was connected to the chipboard via an FMC (FPGA Mezzanine Card) cable. A 10 Gb Ethernet connection between the FPGA and a PC was provided via an optic fiber. The Si sensor was biased to  $-150$  V by a high-voltage source-measure unit (Keithley 237) that was connected to the chipboard via LEMO cable. The biasing current was measured in the order of 10 nA during the experimental campaign. To overcome the sensor readout saturation, one block-wide shield consisting of 5 cm thick Pb blocks was installed in front of the sensor. Additionally, the active window (the number of active pixels in the sensor) was narrowed to reduce the data volume to be read out by the readout system.

#### 4.2 12th RE campaign: November 2020

During the last RE-dedicated campaign conducted in November 2020 at the COMPASS tokamak, the detector setup was similar to the one described above. During the first half of the campaign, the detector was installed at the port with an extension with length of 170 mm and diameter of 52 mm, therefore the sensor was closer to the tokamak vacuum vessel than during the 11th RE campaign. As the RE intensity rose from the start of the campaign, the system readout reached saturation. Limited space between the sensor and the port left no space for sufficient shielding. To keep the detector running, the whole setup was moved from the port to a table approximately four meters away from the tokamak for the rest of the campaign. A shield of one block-wide, 5 cm-thick Pb blocks was added to secure the readout system from reaching saturation and to allow to operate the sensor with all pixels activated. In the block in front of the sensor, a hole was cut out, simulating a pinhole.

## 5 Experiment results

During the 11th RE campaign at the COMPASS tokamak, Timepix3 had successfully measured 49 shots out of approx. 150 total. As these were one of the first shots for the Timepix3 in a tokamak environment, the detector has met multiple obstacles, mainly the saturation of the readout system. However, the data collected are in good correlation with the signals from the diagnostics that are routinely used in RE-dedicated experiments. The plasma current measured by a Rogowski coil,

HXR from the NaI(Tl) scintillation detector, and a neutron and HXR signal from the EJ-410 detector was mainly used for comparison. Figure 2 shows the signals from shot 20055 for all diagnostics mentioned. The shot was conducted with an Ar puff which resulted in a disruption at 1357.05 ms. A strong spike in both HXR and SXR signals and a rapid drop in the plasma current can be seen at that moment. Weak HXR and SXR signals after the disruption indicate, arguably, a short-lived RE beam. In the time interval 1160–1245 ms, the plasma survived a minor instability, which is seen in the ripples in the plasma current and spikes in the SXR signal from the Timepix3, see figure 3. It is worth mentioning that while the SXR signal compared to the HXR ones may appear zero during the initial phase of the shot, it is actually very weak with approximately  $60 \text{ hits ms}^{-1}$  detected from the start until the gas puff. This figure shows that the Timepix3 detector is not only capable of measuring secondary RE radiation but also is much more sensitive to minor instabilities than the HXR diagnostics.

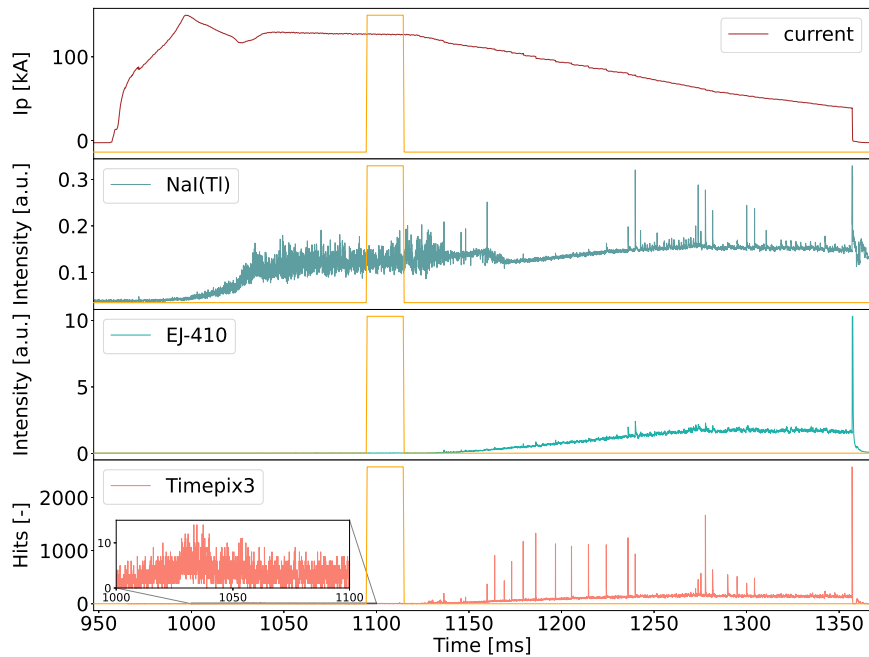


**Figure 2.** Shot 20055, plasma current, HXR signal from NaI(Tl), neutron and HXR signal from EJ-410, and a SXR signal from Timepix3. The Ar puff is shown in orange.

Apart from the time evolution of SXR radiation, Timepix3 can be also used as a camera. In figure 4, graphite tiles of the HFS limiter can be seen in a snapshot from the detector. The number of active pixels was lowered down to 12100 to overcome the readout system saturation. The size and the position of the window was chosen as such due to the position of the pinhole, which was seen in a snapshot in a shot with lower RE activity. The figure represents a collection of snapshots from a time interval 950–1100 ms when the RE activity was at the lowest and until the initial REs stopped hitting the HFS tiles due to the change of magnetic configuration. A snapshot from the fast camera also confirms this, see figure 5. The snapshot shown is taken from another shot as in shot 20068 the camera did not record and the snapshot from the Timepix3 from shot 20068 is the best example.

During the 12th RE campaign, Timepix3 collected useful data in 113 shots out of 218 conducted with 29 unsaturated signals collected from the port of the tokamak. Most of the data were collected

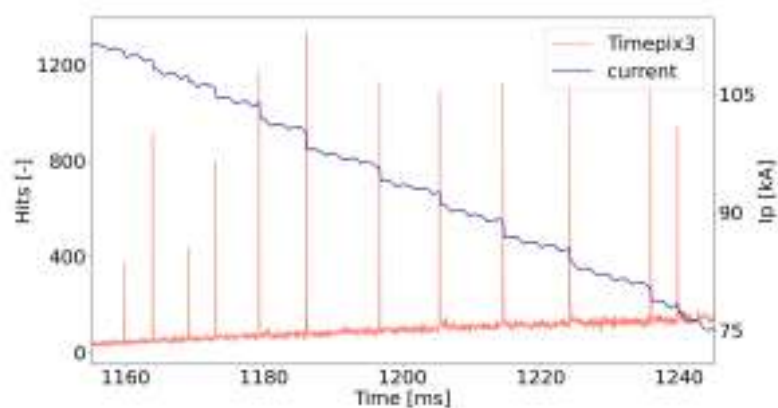


**Figure 3.** Shot 20055, the minor instability that developed after the Ar puff is seen in the ripples in the plasma current and enhanced SXR from REs.

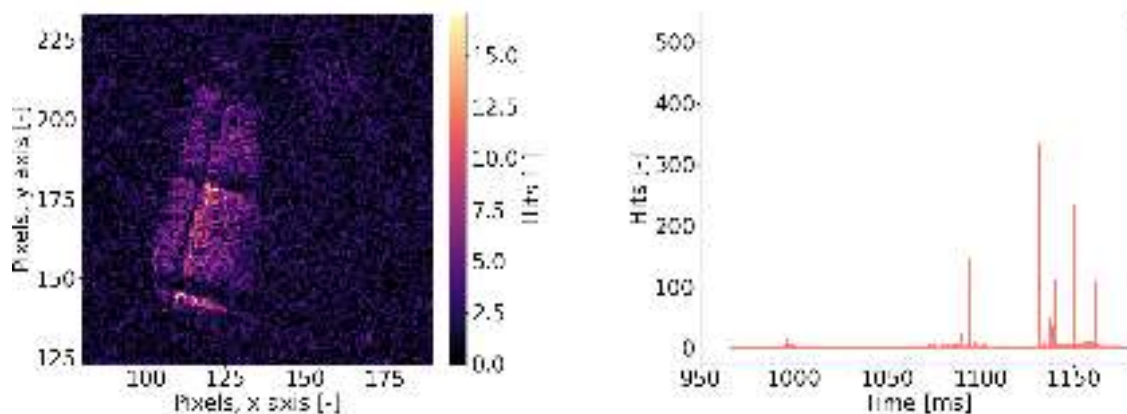


**Figure 4.** Shot 20068. On the left, a collection of sensor snapshots from a time interval 950–1100 ms, on the right, the time evolution of the SXR signal from the Timepix3 detector is shown.



**Figure 5.** On the left, interior of the COMPASS tokamak vacuum chamber [18], on the right, shot 20056, snapshot taken at 991.3 ms from the fast camera Photron Mini UX100 operated at 6.25 kfps.

while the detector was approximately four meters away from the vacuum chamber. In this setup, however, the detector lost its usefulness as a camera. Nonetheless, the measurements were successful with interesting results that lead to a more in-depth data analysis. In figure 6, a comparison between the Timepix3 and the scintillation detectors signals is shown. Two strong peaks in both neutron and SXR signals can be seen at the time 1219 ms and 1312 ms, when the shot has terminated in a disruption. Both peaks indicate a loss of control of the RE beam which hit the wall, resulting in a production of photoneutrons and an enhanced emission of X-rays. Similar to shot 20055, the plasma survived a minor instability which is seen in the ripples in the plasma current and enhanced X-ray signals. This time, however, the SXR signal shows periodic oscillations.

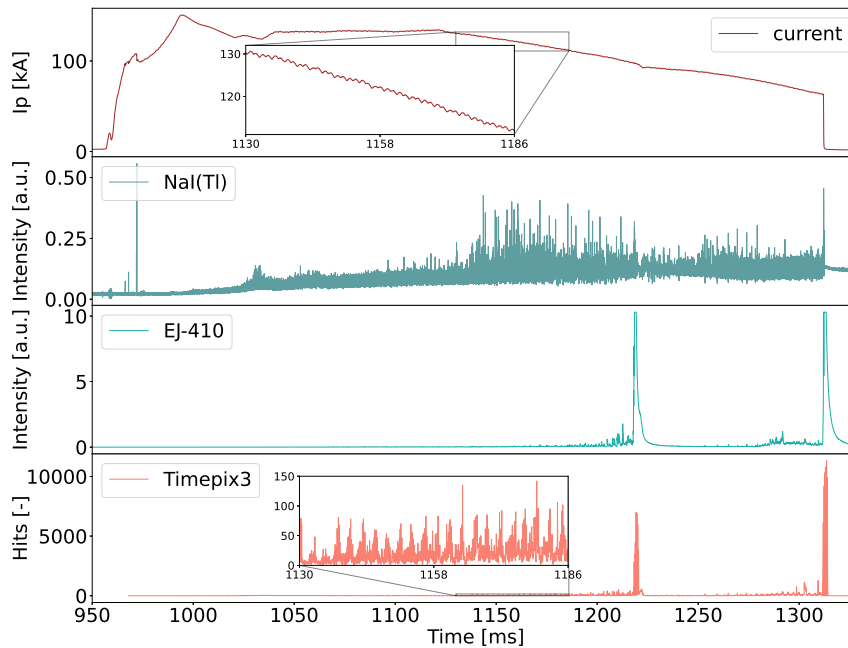


**Figure 6.** Shot 21213, plasma current, HXR signal from NaI(Tl), neutron and HXR signal from EJ-410, and SXR signal from Timepix3.

To investigate the nature behind the periodicity seen in the SXR signal, a spectrogram of signals from a Mirnov coil and Timepix3 was calculated, see figure 7. The first spectrogram shows magnetic activity of the plasma which affects the RE radiation, which can be seen in the second spectrogram. Similar correlations have been previously seen at the COMPASS tokamak between the HXR intensity and magnetic activity of the plasma [19]. Periodic oscillations, such as in shot 21213, have been discovered in almost all SXR signals, including shots from the 11th RE campaign. Investigation of this phenomenon is still ongoing. Theoretically, Timepix3 can provide more information on the nature behind these correlations as it can be placed closer to the plasma than NaI(Tl) detectors, providing more local measurements. However, how plasma magnetic activity affects the RE losses should be studied in the shots with lower RE intensity. Otherwise, the Timepix3 readout system is likely to saturate if the detector is close to the tokamak.

Besides the original readout rate at  $40 \text{ Mhits s}^{-1}$ , the SPIDR readout system has also added a possibility to operate the detector at  $80 \text{ Mhits s}^{-1}$ . The faster configuration was successfully tested during



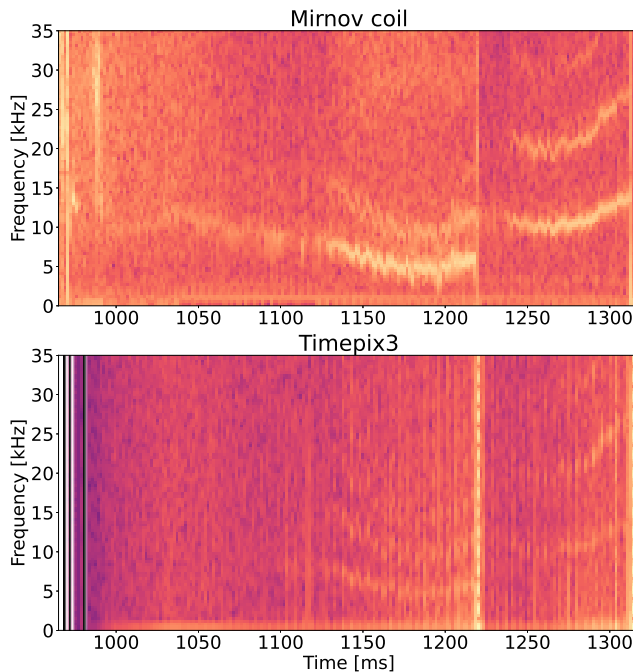


**Figure 7.** Shot 21213, spectrograms of a Mirnov coil signal and the SXR signal from Timepix3.

the 12th RE campaign. While the data collected were good, the sensor snapshots showed increased noise in some of the pixels. In June 2021, the setup was sent to Nikhef for further investigation.

## 6 Energy measurements and calibration of the Timepix3

Additional to recording the time evolution of the incoming SXR and serving as a camera, Timepix3 is also capable of recording the energy deposited in the sensor — the ToT signal. The signal itself, however, is binary encoded and an energy calibration is required to get V or eV. The calibration can be conducted either by measuring radiation sources with known energy yield or via a charge injection method. One should not forget that the matrix of  $256 \times 256$  pixels requires calibration of each individual pixel separately as each one responds somewhat differently.

In the charge injection method, a pulse of increased voltage is generated in each pixel and their response is recorded. To avoid cross-talk, injection is conducted in only 1000 pixels simultaneously. In total, each pixel measures 100 pulses and the mean value of the measured 100 responses is taken. Next, all mean ToT values are taken as a function of the voltage injected (that means 65536 ToT values per injected pulse amplitude) and are fitted using the function [20]:

$$f_{\text{tot}}(x) = a_{\text{tot}}x + b_{\text{tot}} - \frac{c_{\text{tot}}}{x - t_{\text{tot}}}, \quad (6.1)$$

where  $x$  is the voltage injected. The fit parameters  $a_{\text{tot}}$ ,  $b_{\text{tot}}$  (gain and offset of the linear part of the response measured),  $c_{\text{tot}}$ , and  $t_{\text{tot}}$  (curvature and asymptote of the non-linear part) are stored separately. In the first order approximation, this function describes the non-linear binary-coded response of the pixels on the applied voltage very well. The non-linear response is caused by the so-called timewalk effect appearing mainly due to the chip architecture. The four fit parameters are

then used to convert the binary-coded ToT values measured during experiments to V. The function used for conversion is the inverse function of 6.1:

$$f_{\text{tot}}^{-1}(x) = \frac{a_{\text{tot}}t_{\text{tot}} + x - b_{\text{tot}} + \sqrt{(b_{\text{tot}} + a_{\text{tot}}t_{\text{tot}} - x)^2 + 4a_{\text{tot}}c_{\text{tot}}}}{2a_{\text{tot}}}, \quad (6.2)$$

where  $x$  is the binary-coded ToT. To get eV, one has to multiply by  $3 \times 10^{-15} \cdot 1.6^{-1} \times 10^{19} \cdot 3.65$  eV, where  $3 \times 10^{-15}$  F is the capacitor value, through which the injection is conducted, 3.65 eV is the mean energy required for the generation of an electron-hole pair in Si.

The result after the calibration via charge injection method for shot 20055 can be seen in figure 8.

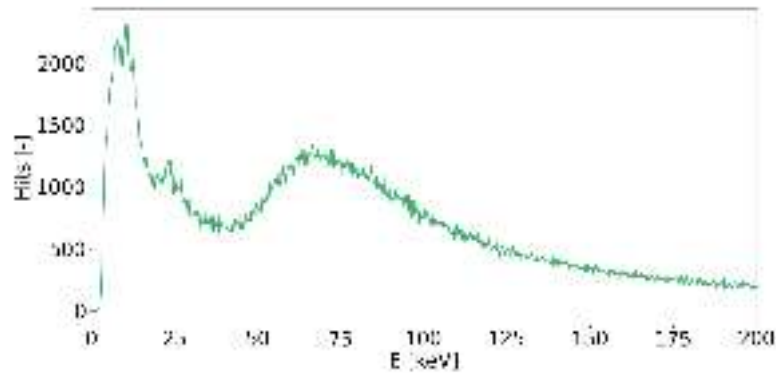


**Figure 8.** Shot 20055, the calibrated ToT signal generated by SXR.

Combining the ToT and ToA signals, one can plot a 2D histogram that provides information about how many photons with a particular energy at a certain time were measured, see figure 9.

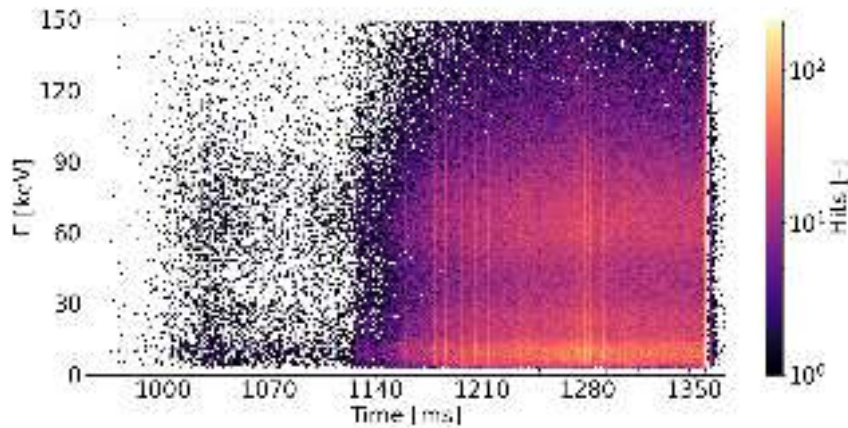


**Figure 9.** Shot 20055, energy calibrated ToT signals plotted versus time.

It is worth mentioning that the calibration conducted has yet unsolved issues. For example, some of the fit parameters calculated from 6.1 have large deviations: the  $c_{\text{tot}}$  parameter has a value from 0 up to 250000. Furthermore, plotting a 2D histogram of each parameter shows striped patterns, see figure 10. The reasons behind this are yet uncovered and further investigation is required.

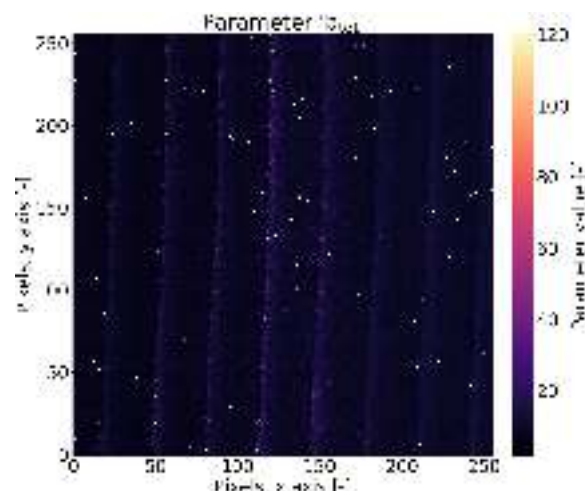


**Figure 10.** Fit parameter  $b_{\text{tot}}$  as function of position in the pixel matrix, showing stripe patterns.

## 7 Experiments at the GOLEM tokamak

In May 2021, the Timepix3 detector was installed at the GOLEM tokamak, which is located at the Faculty of Nuclear Sciences and Physical Engineering of the Czech Technical University in Prague [21]. The main idea behind the experiments was to test the automation of the data acquisition system. During both the 11th and 12th RE campaigns at the COMPASS tokamak, the Timepix3 detector was operated manually. After the campaigns, the data acquisition and the data analysis systems were automated via a package of scripts written in Python. The scripts were integrated into the GOLEM tokamak system, running system preparation, starting the data acquisition, conducting the data analysis, and preparing plots according to the status of the shot. During the experiments, however, the detector was damaged: the sensor bonding was destroyed and the sensor itself got detached from the chip. While there is no useful data to show, as it were the first few days of the first experiments, after a long pause at the tokamak, the data acquisition automation worked as designed. The Timepix3 was sent back to Nikhef for repair. In the future, the detector will accompany the RE diagnostics at the GOLEM tokamak.

## 8 Conclusion

The Timepix3 detector was tested in a tokamak environment in RE-dedicated campaigns at the COMPASS tokamak. Different setups and configurations were tested. The time evolution signals are well correlated with the ones routinely used in RE experiments diagnostics - the NaI(Tl) scintillation detector and the EJ-410 fast neutron detector. Besides that, Timepix3 can be used as a camera, either for observations of interactions between REs and plasma-facing components or, theoretically, between REs and either MGI or SPI. During the 12th RE campaign, the detector was also tested in a setup in which scintillation detectors usually run: a couple of meters away from the vacuum chamber. While in this setup Timepix3 loses its usefulness as a camera, it still can be run as a SXR detector.

Additionally, a calibration via the charge-injection method was conducted. While due to the yet unsolved and not yet fully understood issues the calibrated ToT signals are not accurate, the data presented still serves as an example of what the Timepix3 detector is capable of.

A more detailed analysis of the time evolution signals, which show periodic oscillations, discovered a correlation between the plasma magnetic activity and RE-generated radiation. The investigation into the nature behind these correlations is ongoing.

In a short experimental campaign, the detector was also tested at the GOLEM tokamak where an automated data acquisition and analysis system was tested with success. In the future, this will help with running the detector on its own.

To summarize, the Timepix3 detector is a suitable diagnostic not only for RE-dedicated experiments, but SXR measurements in tokamaks in general. Changing the material and width of the sensor, it is possible to adapt the diagnostic for measurements of HXR and neutrons. Thanks to the pixel size of  $55 \times 55 \mu\text{m}$ , the system has great spatial resolution with data readout in the order of ns. Additionally, because of the pixel matrix and the readout chip architecture, the system can withstand high radiation fluxes. For now, the Timepix3 detector still requires more time and tests to fully assess its capabilities and, therefore, it is considered as an addition to plasma diagnostics. The key problem the system met during the experiments is the saturation of the readout system. In theory, this should be countered with the use of sufficient shielding and faster readout at  $80 \text{ Mbits s}^{-1}$ . However, the necessity of shielding may interfere with the compact dimensions of the detector, making the installation closer to the vacuum chamber trickier. In the case installation close to the chamber is impossible, the system still can be utilized as an X-ray detector (in the case of Si sensor), essentially losing only its usability as a camera. The system combines several diagnostics, making a compact, fast, reliable, and fully automated tool for plasma diagnostics.

## Acknowledgments

This work was supported by the project / is part of the project / of Ministry of Education, Youth and Sports of the Czech Republic; Centre of Advanced Applied Sciences CZ.02.1.01/0.0/0.0/16\_019/0000778 co-financed by the European Union and by the Grant Agency of the Czech Technical University in Prague, grant No. SGS21/167/OHK4/3T/14, co-funded by MEYS project LM2018117 and by the Dutch Research Council (NWO).

## References

- [1] H. Dreicer, *Electron and Ion Runaway in a Fully Ionized Gas. II*, *Phys. Rev.* **117** (1960) 329.
- [2] T. Hender, J. Wesley, J. Bialek, A. Bondeson, A. Boozer, R. Buttery et al., *Chapter 3: MHD stability, operational limits and disruptions*, *Nucl. Fusion* **47** (2007) S128.
- [3] Z.Y. Chen, W.C. Kim, Y.W. Yu, A.C. England, J.W. Yoo, S.H. Hahn et al., *Study of runaway current generation following disruptions in KSTAR*, *Plasma Phys. Control. Fusion* **55** (2013) 035007.
- [4] J.R. Martín-Solís, B. Esposito, R. Sánchez, F.M. Poli and L. Panaccione, *Enhanced Production of Runaway Electrons during a Disruptive Termination of Discharges Heated with Lower Hybrid Power in the Frascati Tokamak Upgrade*, *Phys. Rev. Lett.* **97** (2006) 165002.
- [5] R.E. Jaspers, *Relativistic runaway electrons in tokamak plasmas*, Ph.D. thesis, Technische Universiteit Eindhoven (1995).

- [6] J. Mlynar, O. Ficker, E. Macusova, T. Markovic, D. Naydenkova, G. Papp et al., *Runaway electron experiments at COMPASS in support of the EUROfusion ITER physics research*, *Plasma Phys. Control. Fusion* **61** (2018) 014010.
- [7] J. Mlynar, O. Ficker, M. Vlainic, V. Weinzettl, M. Imrisek, R. Paprok et al., *Effects of plasma control on runaway electrons in the COMPASS Tokamak*, in proceedings of the 42<sup>nd</sup> EPS Conference on Plasma Physics, Lisbon, Portugal, 22–26 June, 2015, vol. 39, European Physical Society, 2015 [<http://ocs.ciemat.es/EPS2015PAP/pdf/P4.102.pdf>].
- [8] R.S. Granetz, B. Esposito, J.H. Kim, R. Koslowski, M. Lehnen, J.R. Martin-Solis et al., *An ITPA joint experiment to study runaway electron generation and suppression*, *Phys. Plasmas* **21** (2014) 072506.
- [9] The ITER Organisation, *ITER Research Plan Within the Staged Approach (Level III–Provisional Version)*, Tech. Rep., ITR-18-003, 2018 [[https://www.iter.org/doc/www/content/com/Lists/ITER\\_Technical\\_Reports/Attachments/9/ITER\\_Research\\_Plan\\_within\\_the\\_Staged\\_Approach\\_levIII\\_provversion.pdf](https://www.iter.org/doc/www/content/com/Lists/ITER_Technical_Reports/Attachments/9/ITER_Research_Plan_within_the_Staged_Approach_levIII_provversion.pdf)].
- [10] E.M. Hollmann, P.B. Aleynikov, T. Fülöp, D.A. Humphreys, V.A. Izzo, M. Lehnen et al., *Status of research toward the ITER disruption mitigation system*, *Phys. Plasmas* **22** (2015) 021802.
- [11] The ITER Organisation, *A Task Force to Face the Challenge*, Iter Newslines, <https://www.iter.org/newsline/-/3183>, 2018.
- [12] M. Lehnen and S. Maruyama, *ITER Disruption Mitigation Workshop*, ITER HQ, 8–10 March 2017 [[https://www.iter.org/doc/www/content/com/Lists/ITER\\_Technical\\_Reports/Attachments/8/ITER\\_Disruption\\_Mitigation\\_Workshop.pdf](https://www.iter.org/doc/www/content/com/Lists/ITER_Technical_Reports/Attachments/8/ITER_Disruption_Mitigation_Workshop.pdf)].
- [13] P. Vondracek, R. Panek, M. Hron, J. Havlicek, V. Weinzettl, T. Todd et al., *Preliminary design of the COMPASS upgrade tokamak*, *Fusion Eng. Des.* **169** (2021) 112490.
- [14] Institute of Plasma Physics, *COMPASS Tokamak*, [http://www.ipp.cas.cz/vedecka\\_struktura\\_ufp/tokamak/COMPASS/](http://www.ipp.cas.cz/vedecka_struktura_ufp/tokamak/COMPASS/).
- [15] V. Weinzettl, R. Panek, M. Hron, J. Stockel, F. Zacek, J. Havlicek et al., *Overview of the COMPASS diagnostics*, *Fusion Eng. Des.* **86** (2011) 1227.
- [16] T. Poikela, J. Plosila, T. Westerlund, M. Campbell, M.D. Gaspari, X. Llopart et al., *Timepix3: a 65K channel hybrid pixel readout chip with simultaneous ToA/ToT and sparse readout*, *2014 JINST* **9** C05013.
- [17] J. Visser, M.v. Beuzekom, H. Boterenbrood, B.v.d. Heijden, J.I. Muñoz, S. Kulis et al., *SPIDR: a read-out system for Medipix3 & Timepix3*, *2015 JINST* **10** C12028.
- [18] J. Adamek, *COMPASS tokamak chamber*, [https://commons.wikimedia.org/wiki/File:COMPASStokamak\\_chamber.jpg](https://commons.wikimedia.org/wiki/File:COMPASStokamak_chamber.jpg).
- [19] O. Ficker, J. Mlynar, M. Vlainic, J. Cerovsky, J. Urban, P. Vondracek et al., *Losses of runaway electrons in MHD-active plasmas of the COMPASS tokamak*, *Nucl. Fusion* **57** (2017) 076002.
- [20] F.M. Pitters, N. Alipour Tehrani, D. Dannheim, A. Fiergolski, D. Hynds, W. Klempt et al., *Time and Energy Calibration of Timepix3 Assemblies with Thin Silicon Sensors*, Tech. Rep., CLICdp-Note-2018-008, CERN, Geneva (2018).
- [21] V. Svoboda, B. Huang, J. Mlynář, G. Pokol, J. Stöckel and G. Vondrášek, *Multi-mode remote participation on the GOLEM tokamak*, *Fusion Eng. Des.* **86** (2011) 1310.